13 Rock dynamics and time dependency

13.1 Strain rates

Rock behaviour mechanisms can occur at significantly different rates: during the excavation of rock using explosives, rock failure occurs in milliseconds; a rock block can slip out of a cavern roof in a second; a shaft might take a day to fill up with water; a chalk or mudstone face can deteriorate in a few days. It may take months or years for water to move through a granitic rock mass and, during the 120 years design life of an unlined rock cavern for civil engineering purposes, creep processes could lead to roof collapse. Some geological processes occur over millions of years.

In view of this time dependency over a wide time range, it is convenient to consider the rate at which such processes occur in terms of strain rate. Consider a rock cylinder subjected to uniaxial compression along its axis and that the rock's compressive strength is reached at 0.5% strain, i.e. 0.005 or 5×10^{-3} strain. At a **strain rate** of 1×10^{-3} s^{-1}, the rock specimen will fail in 5 s. At a strain rate of 1×10^{-4} s^{-1}, the rock specimen will fail in 50 s. For explosive failure in 2 ms, the strain rate would be $5 \times 10^{-3}/2 \times 10^{-3} = 2.5$ or 2.5×10^{0} s^{-1}. Note that there are four orders of magnitude difference between the slowest and fastest of these examples.

A range of strain rates is shown in Fig. 13.1. These are the strain rates per second, and above the strain rate scale some failure times for the rock specimen are shown.

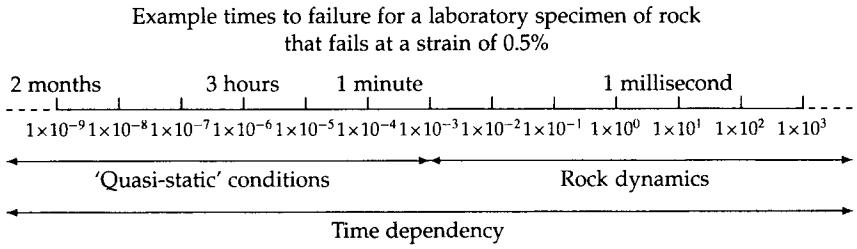

Figure 13.1 Range of strain rates

The distinction between 'quasi-static' and 'dynamic' shown in Fig. 13.1 is arbitrary, although the realm of rock dynamics is usually regarded as being those strain rates at which '**quasi-static**' laboratory tests are impractical and where vibrations will occur, above, say, 1×10^{-3} s^{-1}. Note, however, that the phenomenon of time dependency occurs over the full spectrum of strain rates.

We emphasized in ERM 1, and in the questions in earlier chapters of this book, that there is no time component in elasticity: the relations between stress and strain are not a function of time. Hence, rather than say that elasticity occurs at an infinite strain rate, it is better to say that elasticity is independent of time. However, for the high strain rates, we can discuss the velocities of **propagation of stress waves** in elastic rocks, which can be determined as a consequence of Hooke's Law and the equations of motion. In A3.11 we showed that the sum of the rates of changes of the stress components in a given direction is zero when no force is applied, e.g. $\frac{\partial \sigma_{xx}}{\partial x} + \frac{\partial \tau_{yx}}{\partial x} + \frac{\partial \tau_{zx}}{\partial x} = 0$. When the sum of these rates of change is not zero (meaning that a net force is applied), then force = mass × acceleration, or $\frac{\partial \sigma_{xx}}{\partial x} + \frac{\partial \tau_{yx}}{\partial x} + \frac{\partial \tau_{zx}}{\partial x} = \rho \frac{\partial^2 u}{\partial t^2}$. This is for equilibrium in the x-direction, where ρ is the rock density and u is displacement in the x-direction.

Considering a one-dimensional situation, for example, stress waves travelling along a rod, this equation of motion reduces to $\frac{\partial \sigma_{xx}}{\partial x} = \rho \frac{\partial^2 u}{\partial t^2}$. Because $E = \frac{\text{stress}}{\text{strain}} = \sigma_{xx} \Big/ \left(\frac{\partial u}{\partial x}\right)$, $\sigma_{xx} = E \frac{\partial u}{\partial x}$, and hence $E \frac{\partial^2 u}{\partial x^2} = \rho \frac{\partial^2 u}{\partial t^2}$. Rearranging this gives $\frac{E}{\rho} = \frac{\partial^2 u}{\partial t^2} \cdot \frac{\partial^2 x}{\partial u^2} = \rho \frac{\partial^2 u}{\partial t^2}$, which shows that this relation corresponds to a **longitudinal stress wave** velocity of $V_p = \sqrt{\frac{E}{\rho}}$.

In the two-dimensional case for an isotropic material, the longitudinal velocity in a plate is $V_p = \sqrt{\frac{E}{\rho(1-\nu^2)}}$, and in three dimensions, $V_p = \sqrt{\frac{E(1-\nu)}{\rho(1-2\nu)(1+\nu)}}$. The longitudinal stress waves are also referred to as dilatational, compressive, or primary waves.

The **transverse stress wave**, which has a different velocity from the longitudinal stress wave, can also be referred to as a distortional, shear, or secondary wave. There are also longitudinal surface (or Rayleigh) waves, transverse surface (or Love) waves, and Stoneley waves which occur at the boundary of two connected elastic rock strata.

There is a variety of **time-dependent effects** at lower strain rates. **Creep** occurs when the stress is held constant and the strain changes. **Relaxation** occurs when the strain is held constant and the stress changes. **Fatigue**

occurs when there is increasing strain during stress cycling. When the complete stress–strain curve is obtained in uniaxial compression at strain rates of, for example, 1×10^{-3} s^{-1}, 1×10^{-4} s^{-1}, and 1×10^{-5} s^{-1}, the results will be strain rate-dependent: the compressive strength might be 20% higher at a strain rate of 1×10^{-3} s^{-1} compared to the compressive strength obtained at a strain rate of 1×10^{-5} s^{-1}; and the shape of the post-peak curve will be influenced by time-dependent processes.

Thus, time-dependent phenomena are important for both the discipline of rock mechanics and the rock engineering applications. Many rocks exhibit significant time dependency, yet we do not have such comprehensive methods of characterizing and predicting time-dependent behaviour as compared to either elastic or plastic behaviour.

13.2 Questions and answers: rock dynamics and time dependency

Q13.1 There is no time component in the theory of elasticity. Why then does Young's modulus, expressed in units of stress, have time in its dimensions: $L^{-1}MT^{-2}$?

A13.1 Although it is correct that the relation between stress and strain is independent of time, the units contain the time dimension because stress is defined as force/area and force is defined using Newton's second law which contains acceleration. Young's modulus is expressed as E = stress/strain = (F/A)/strain = (kg m s^{-2}/m^2)/strain = kg m^{-1} s^{-2}/strain, and hence we see that Young's modulus involves time. The dimensions of Young's modulus are $L^{-1}MT^{-2}$, as given in the units section at the beginning of this book.

The SI force unit, the newton, is defined as the force required to accelerate a mass of one kilogram at a rate of one metre per second per second — hence involving time. Note that all derived SI units are developed via some physical relation using the three base units of metre, kilogram and second.

Q13.2 A 10-mm-diameter core of intact marble is carefully drilled out to a length of 1 m. The core is suspended horizontally by steel wires and then struck gently at one end to produce a longitudinal stress wave through the bar, as shown below. This is known as the Hopkinson bar experiment, used to study the transmission of stress waves.

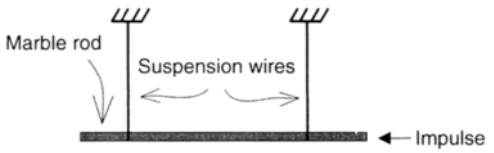

(a) If Young's modulus of the marble is 50 GPa and the unit weight is 27 kN/m^3, estimate the time taken for the longitudinal stress wave to travel from one end of the core to the other.

(b) Given that marble has a sufficiently high compressive strength to sustain the compressive wave but has a low tensile strength, where will the bar break, and why?

A13.2 (a) We assume that the longitudinal velocity in the core is given by $V_p = \sqrt{E/\rho}$, where E is Young's modulus and ρ is the density. For a unit weight of 27 kN/m^3 and an acceleration due to gravity of 10 m/s^2, the density is $27 \times 10^3/10 = 2700$ kg/m^3. Thus, we find $V_p = \sqrt{50 \times 10^9/2700} = 4300$ m/s. As the bar has a length of 1 m, the wave will therefore take $1/4300 = 2.32 \times 10^{-4}$ s, or 232 μs to travel along it.

(b) The compressive wave travels down the core but is reflected at the free end as a tensile wave.

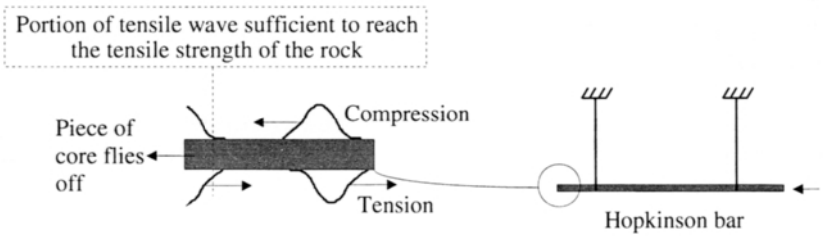

Once the absolute amplitude of the reflected tensile wave is sufficiently greater than the absolute amplitude of the incident compressive wave, the tensile strength will be reached and a piece will fly off the end of the length of core.

Q13.3 **What is the ratio V_p^2/V_s^2 in terms of the elastic rock constants and what is the specific value of the expression for a rock with $\nu = 0.27$?**

A13.3 We have $V_p = \sqrt{E(1-\nu)/\rho(1-2\nu)(1+\nu)}$ and $V_s = \sqrt{E/2\rho(1+\nu)}$, and so $V_p^2/V_s^2 = 2(1-\nu)/(1-2\nu)$. This is a useful relation for seismic rock mass investigations enabling easier evaluation of the dynamic elastic constants. For a rock with $\nu = 0.27$, $V_p^2/V_s^2 = 2(1-0.27)/(1-0.54) = 3.174$. Thus, we see that longitudinal waves propagate faster than shear waves.

If the density is known, Poisson's ratio can be estimated from V_p^2/V_s^2 and then the dynamic Young modulus estimated from V_p. Also, the relations between V_p, V_s and the elastic constants mean that rock masses can be classified using the values of V_p and V_s.

Q13.4 **A 100-mm-long rock specimen is to be tested in uniaxial compression using strain control in a servo-controlled testing machine. The Young's modulus of the rock is 60 GPa and the compressive strength is 200 MPa. We should like to reach the compressive strength in the test in about 10 minutes. What displacement rate should be used for the testing machine program, and what is the corresponding rock strain rate?**

A13.4 Firstly, we have to calculate the rock specimen displacement at the compressive strength. The strain at the compressive strength

is stress/E = 200/60000 = 0.0033. For a specimen 100 mm long, this is 100 × 0.0033 = 0.33 mm displacement. To reach this displacement in 10 minutes requires a displacement rate of 0.33/600 mm/s = 0.00055 mm/s or 5.5×10^{-7} m/s. This is equivalent to a strain rate of 0.00055/100 per s = 0.0000055 s^{-1} = 5.5×10^{-6} s^{-1}.

The displacement rate used in practice would have to be slightly faster than the calculated value of 5.5×10^{-7} m/s because the stress–strain curve will have a lower slope than 60 GPa both in the initial portion, when 'bedding down' occurs, and near the peak stress, when cracking occurs.

***Q13.5* The results in the table below show the axial displacement and radial strain induced in a cylindrical specimen of weak chalk during a uniaxial creep test. In this test, the specimen was initially 250 mm high and was subjected to an axial stress of 55 MPa. After 3 hours the test was stopped, at which stage creep had ceased and the displacement had become constant at 0.4545 mm.**

Time (min):	**0**	**1**	**2**	**3**	**4**	**5**	**6**	**7**
Axial displacement (mm):	**0.409**	**0.414**	**0.419**	**0.423**	**0.427**	**0.430**	**0.433**	**0.435**
Radial strain ($\times 10^{-6}$):	**−451**	**−461**	**−471**	**−479**	**−487**	**−493**	**−499**	**−504**
Time (min):	**8**	**9**	**10**	**11**	**12**	**13**	**14**	**15**
Axial displacement (mm):	**0.438**	**0.440**	**0.441**	**0.443**	**0.444**	**0.445**	**0.447**	**0.447**
Radial strain ($\times 10^{-6}$):	**−509**	**−513**	**−516**	**−519**	**−522**	**−524**	**−526**	**−528**

On the basis of these results, select a simple viscoelastic model for the rock, and determine values for the various viscoelastic constants.

A13.5 Simple viscoelastic models are built up from elastic (spring) and viscous (dashpot) elements connected in series, parallel or a combination of both. In order to decide on a likely model, we start by computing the axial strain from these data, and then plotting the results (see next page) in order to visualize the behaviour of the specimen.

Time (min):	0	1	2	3	4	5	6	7	
Axial strain ($\times 10^{-3}$):	1.635	1.656	1.675	1.692	1.707	1.720	1.731	1.742	
Time (min):	8	9	10	11	12	13	14	15	180
Axial strain ($\times 10^{-3}$):	1.751	1.759	1.766	1.772	1.777	1.782	1.786	1.790	1.818

From this we see that the specimen displays an immediate elastic response when the axial stress is applied, indicating that the viscoelastic model we choose must have an elastic element directly in series with the applied stress. Also, because the viscous creep of the material stops after a definite time, then the viscous element must be connected in parallel

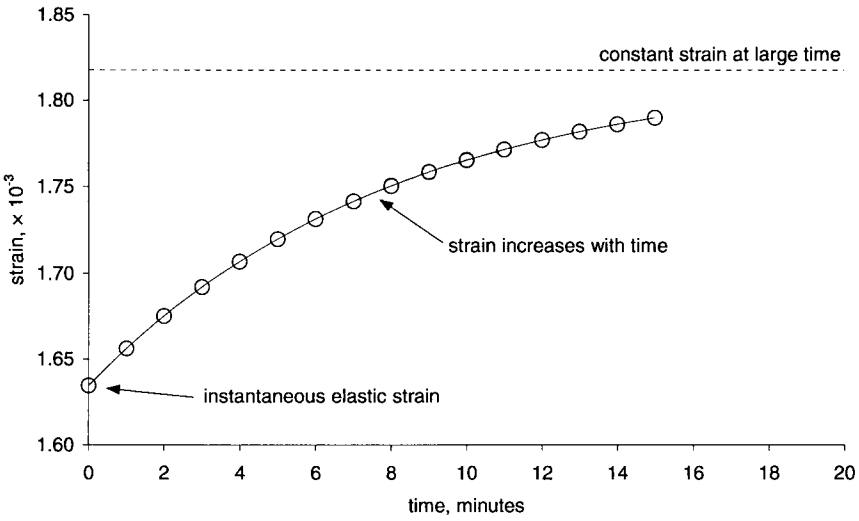

with another spring element. Assembling these elements results in a generalized Kelvin material, which is shown schematically below.

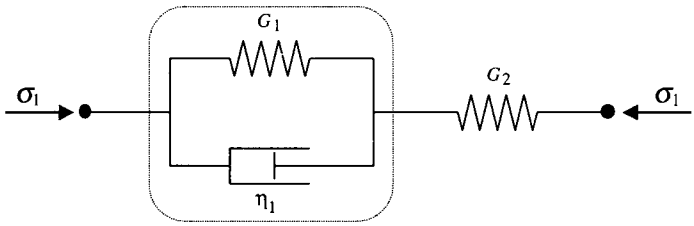

In this model, the elastic element with stiffness G_2 is responsible for the immediate elastic response. If we consider the part of the model within the dotted line, then immediately after the loading is applied the stress is borne by the viscous element, but as time passes the stress is eventually borne entirely by the elastic element. Thus the viscous element, with viscosity η_1, is responsible for the creep and the elastic element, with stiffness G_1, is responsible for causing the creep to cease.

Viscoelastic materials are usually assumed to act elastically when subjected to a hydrostatic stress state (if this were not true, viscoelastic materials would creep when submerged in water), and creep only when subjected to a stress state that causes distortion. For a material that acts as a generalized Kelvin material in distortion and as an elastic material in hydrostatic compression, the constitutive equation for a uniaxial stress state is (Jaeger and Cook, 1979; Goodman, 1989)[1]

$$\varepsilon_1 = \frac{\sigma_1}{3}\left\{\frac{2}{3K} + \frac{1}{G_2} + \frac{1}{G_1}\left[1 - \exp\left(-\frac{G_1 t}{\eta_1}\right)\right]\right\}.$$

[1] Techniques for deriving such constitutive relations are given by Jaeger J. C. and Cook N. G. W. (1979) *Fundamentals of Rock Mechanics*. Chapman and Hall, London, 3rd edn., 593pp. and Goodman R. E. (1989) *Introduction to Rock Mechanics*. Wiley, Chichester, 2nd edn., 562pp.

At $t = \infty$ this reduces to

$$\varepsilon_1(\infty) = \frac{\sigma_1}{3}\left\{\frac{2}{3K} + \frac{1}{G_2} + \frac{1}{G_1}\right\}$$

and so the difference between the long-term strain and the strain developed at time t is

$$\varepsilon_1(\infty) - \varepsilon_1(t) = \Delta\varepsilon = \frac{\sigma_1}{3}\left\{\frac{1}{G_1}\exp\left(-\frac{G_1 t}{\eta_1}\right)\right\}.$$

Rearranging this leads to

$$\ln(\Delta\varepsilon) = -\frac{G_1}{\eta_1}t + \ln\left(\frac{\sigma_1}{3G_1}\right),$$

which is the equation of a straight line, and shows how we can obtain values for G_1 and η_1.

The table below shows the data required to plot this straight line, and the plot is given below.

t (s):	0	60	120	180	240	300	360	420
$\ln(\Delta\varepsilon)$	−25.33	−25.45	−25.58	−25.70	−25.83	−25.95	−26.08	−26.20
t (s):	480	540	600	660	720	780	840	900
$\ln(\Delta\varepsilon)$	−26.33	−26.45	−26.58	−26.70	−26.83	−26.95	−27.08	−27.20

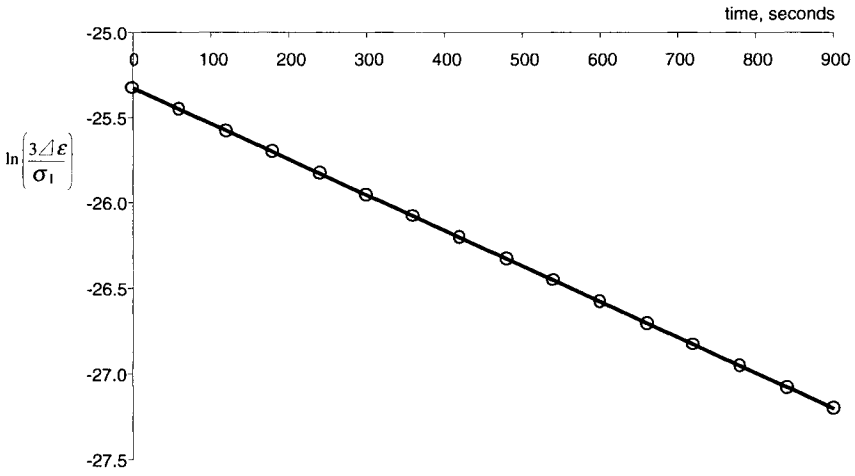

At time $t = 0$ we have

$$\Delta\varepsilon = \frac{\sigma_1}{3G_1}$$

from which we obtain $G_1 = \sigma_1/3\Delta\varepsilon = 55.0 \times 10^6/\left(3 \cdot 1.833 \times 10^{-4}\right) = 100$ GPa. The best-fit straight line through the data has a gradient of -2.083×10^{-3}, from which we obtain

$\eta_1 = G_1/2.083 \times 10^{-3} = 100 \times 10^9/2.083 \times 10^{-3} = 48000$ MPa s.

For small strains the volumetric strain in the uniaxial test may be computed from

$$\varepsilon_V = \varepsilon_1 + 2\varepsilon_3,$$

and so the bulk modulus is given by

$$K = \frac{\text{mean stress}}{\text{volumetric strain}} = \frac{\frac{1}{3}(\sigma_1 + \sigma_2 + \sigma_3)}{\varepsilon_V} = \frac{\sigma_1}{3(\varepsilon_1 + 2\varepsilon_3)}.$$

Rearranging this gives

$$\varepsilon_1 = -2\varepsilon_3 + \frac{\sigma_1}{3K}$$

which shows how the bulk modulus may be found from the intercept of a plot of axial strain versus radial strain. This plot is shown below, and its intercept has been calculated as 733×10^{-6}, from which we obtain $K = \sigma_1/(3 \cdot 733 \times 10^{-6}) = 55 \times 10^6/(3 \cdot 733 \times 10^{-6}) = 25.0$ GPa. Notice that a large amount of extrapolation is required to find the bulk modulus, indicating that this is liable to be an inaccurate technique.

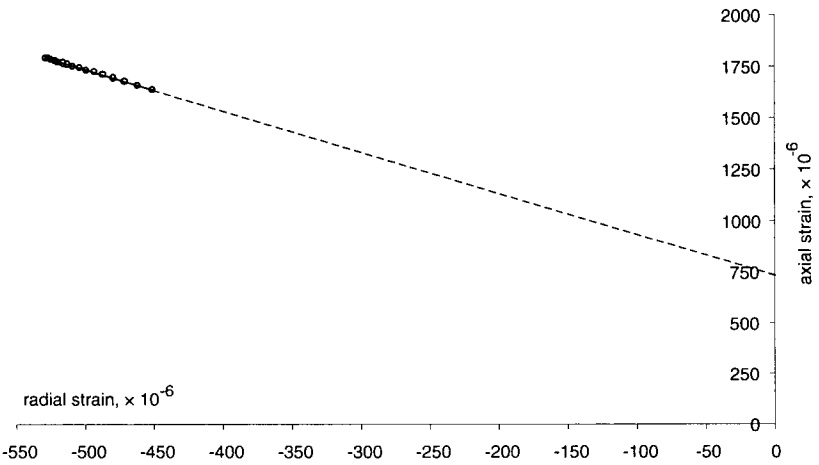

Finally, at $t = 0$ the constitutive equation for the material reduces to

$$\varepsilon_1(0) = \frac{\sigma_1}{3}\left\{\frac{2}{3K} + \frac{1}{G_2}\right\}$$

and rearranging this leads to

$$G_2 = \frac{1}{3\dfrac{\varepsilon_1(0)}{\sigma_1} - \frac{2}{3}\dfrac{1}{K}}$$

from which, by substituting values given above, we obtain $G_2 = 16.0$ GPa.

Q13.6 On a sketch of the complete stress–strain curve for rock in uniaxial compression, draw lines illustrating creep, relaxation and intermediate time-dependent straining along a line of slope $-K$
(a) on the ascending and descending sides of the curve, and
(b) then comment on the significance of your diagram for rock mass stability during time-dependent deformations for a single rock pillar of intact rock and for an abandoned chalk mine excavation (Smith and Rosenbaum, 1993[2]) as shown below.

[2] Smith G. J. and Rosenbaum M. S. (1993) Recent underground investigations of abandoned chalk mine workings beneath Norwich City, Norfolk. *Eng. Geol.*, **36**, 37–78.

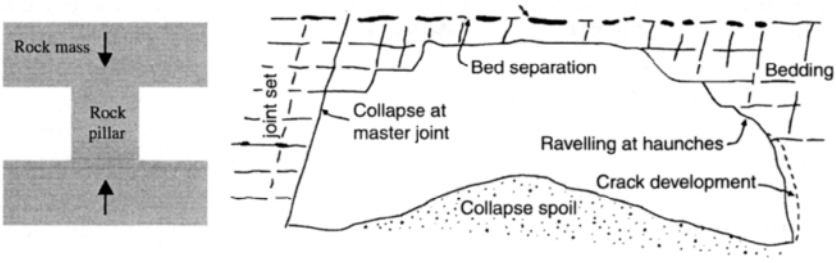

A13.6 (a) Creep is defined as continuing increase in strain at constant stress; relaxation is defined as stress reduction at constant strain. This results in the creep, relaxation and $-K$ lines shown on the diagram below.

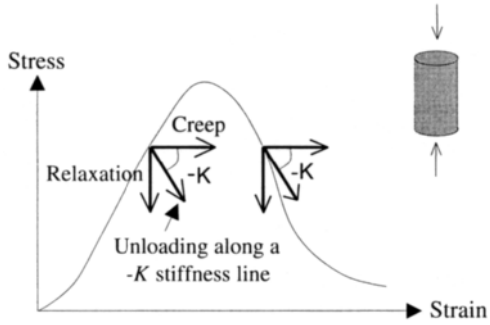

The significance of the diagram for the stability of the two rock masses referred to in the question is that the time-dependent effects of creep, relaxation and intermediate $-K$ creep–relaxation are all stable on the ascending side of the complete stress–strain curve. An exception is when the creep occurs near the top of the curve, so that the rock strains across the stress–strain curve, beneath the peak, to the descending portion whereupon it becomes unstable.

The $-K$ line is important because, in practical cases, the rock mass load is being applied by another part of the rock mass along this line, see sketch to the right. For dead weight loading, $-K$ will be zero, represented by a horizontal line on the stress–strain diagram; if the loading system is rigid, $-K$ tends to infinity, represented by a vertical line.

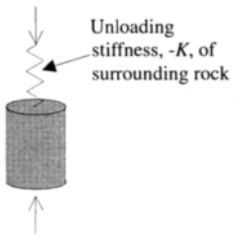

(b) The significance of the diagram for the stability of the two rock masses referred to in the question is that the time-dependent effects of creep and intermediate $-K$ creep–relaxation can lead to sudden collapse, depending on the value of $-K$ and the rock mass condition at any particular point on the complete stress–strain curve. The diagram of the rock pillar shown here was also shown in Q5.10, where the question was whether stress or strain was the cause of rock failure. We see from the $-K$ line in the first diagram above that, with a specified rock mass unloading stiffness, the cause of sudden failure will be a combination of stress and strain. In other words, and as indicated in the sketch on the next page, the failure of the pillar will be

- early and sudden if soft loading is applied, such as through soft rock strata (because the $-K$ line is above the descending portion of the complete stress–strain curve and hence applying more energy than the pillar can absorb as it fails), or
- later and more slowly for stiffer loading, such as through stiff strata, providing explosive phenomena such as rockbursts do not occur (because the $-K$ line will continue to be below the descending portion of the complete stress–strain curve for increasing strain values).

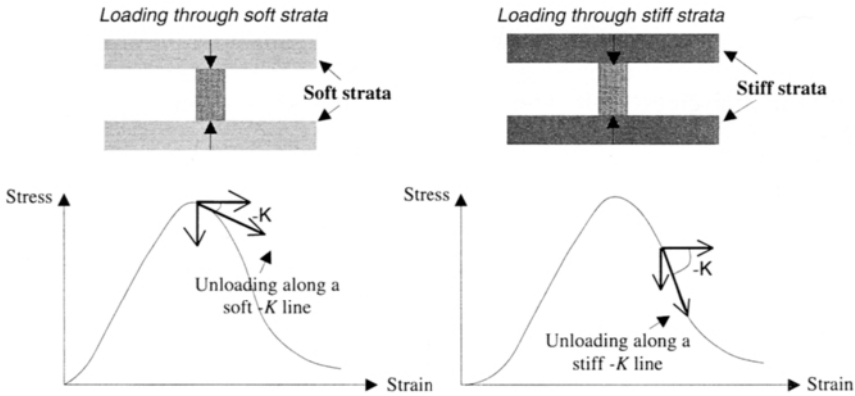

Moreover, such time-dependent effects *in situ* will be exacerbated by general degradation and weathering effects. The diagram to the right in the question illustrates progressive chalk mass deterioration in an underground excavation dating from Victorian times. Here there are several degradation mechanisms operating. The more weathering that occurs in the fractures, the softer and weaker the rock mass will become. Loose blocks fall out, and any bed separation causes the K value to reduce to close to zero. Smith and Rosenbaum also highlight the importance of groundwater flow on the deterioration mechanisms.

Another more general point is that the designers of Victorian rock engineering structures, e.g. for mining or for fresh and waste water systems, could not have anticipated the development of civilization and the current pounding of the ground surface by heavy traffic. So, in addition to all the factors mentioned, there are also the vibrations introduced by modern-day activities, whether as sudden damage due to high-intensity proximate rock blasting or the long-term cumulative effect of vibrations manifested as fatigue failure.

Q13.7 Laboratory fatigue testing results (Ray et al., 1999[3]) for intact Chunar sandstone from the lower Gondwana formation gave the following data.

[3] Ray S. K., Sarkar M. and Singh T. N. (1999) Effect of cyclic loading and strain rate on the mechanical behaviour of sandstone. *Int. J. Rock Mech. Min. Sci.*, **36**, 543–549.

Number of cycles from 0 to 50 MPa	Uniaxial compressive strength (MPa)
0	99.5
100	90.1
200	77.1
300	71.6
400	67.6
500	65.9
600	65.1

The rock samples were cycled for the number of times given in the left-hand column, and then tested for their uniaxial compressive strength, giving the values in the right-hand column.

Plot these results (number of cycles on *x*-axis, *UCS* on *y*-axis) and comment on the trend.

A13.7 As the number of cycles increases, so we see that the strength of the rock decreases. The effect of the cycling is therefore to damage the sandstone through fatigue.

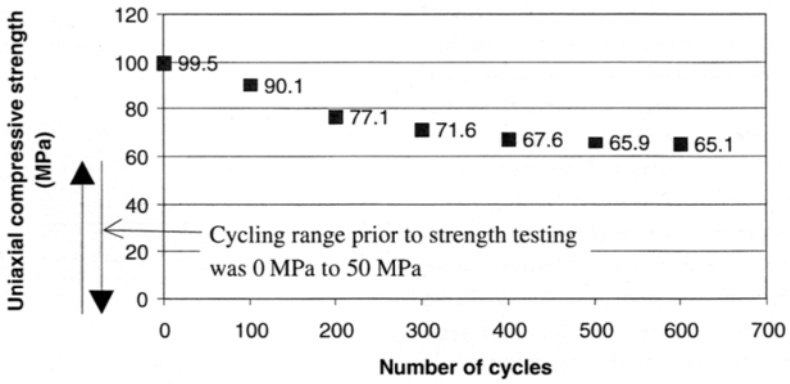

The initial cycles cause the most damage in terms of a percentage strength reduction, and the implication is that the rock is sensitive to such disturbances, despite the low level of stress cycling.

***Q13.8* How do fractures respond to stress waves? What do you think are the influences of a dynamic load on the fracture shear behaviour? What happens if the fractures pictured to the right are subjected to repeated shear movements?**

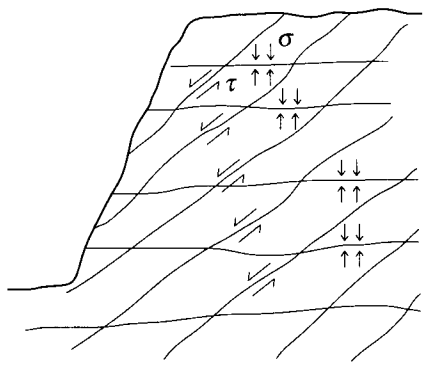

A13.8 Giani (1992)[4] has collated the influences of dynamic loading on fractures. Some of these are:

[4] Giani G. P. (1992) *Rock Slope Stability Analysis*. Balkema, Rotterdam, 361pp.

- shear resistance decreases with the number of forward and reverse fatigue loading cycles (in a directly analogous way to the results given in Q13.7);
- peak shear resistance increases for smooth fracture surfaces with increased loading application frequency;
- the contact area between opposing fracture surfaces increases with contact time;
- the friction angle of weak rocks increases for low normal loads up to a critical loading velocity factor; beyond this value, the friction angle remains constant up to a second critical loading velocity, beyond which shear resistance decreases.

The properties of the fractures in the rock slope will be modified by repeated application of dynamic loads and, in general, the modifications will weaken the rock mass and exacerbate slope instability. However, it is not possible to include all the detailed mechanisms directly into rock engineering design models, which is why we approximate such effects through 'effective rock properties'.

***Q13.9* During the progression of a longwall mining face, bedded rock strata adjacent to the coal mine are being subjected to an extensile strain rate of 1×10^{-5} s^{-1} normal to the bedding planes. Assume that all the strain accumulated in the rock mass is concentrated in opening the bedding planes. How long will it be before the flow of water along the bedding planes is doubled?**

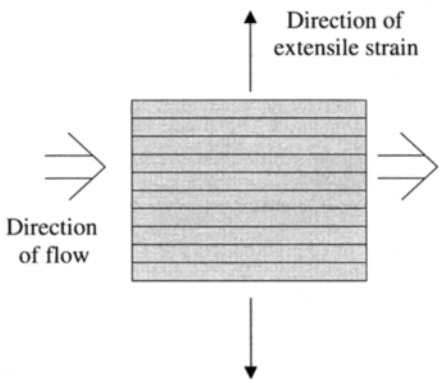

A13.9 Using the cubic law for water flow, we can assume that the flow of water is proportional to the cube of the bedding plane apertures. Then, for an initial aperture of e_i and a final aperture of ce_i, $(ce_i)^3 = 2(e_i)^3$, from which we find $c^3 = 2$ and hence $c = 1.26$. Thus, the aperture must increase in size from a value of 1 unit to a value of 1.26 units — in other words, the strain has to be 0.26 which will occur in
$0.26/1 \times 10^{-5}$ s $= 26000$ s $= 7.2$ h.

***Q13.10* The diagram (Tan, 1993)[5] on the next page illustrates deformations in two mine rail tunnels (originally horseshoe-shaped) in China, which are located at 430 m depth in strongly fractured granite.**

[5] from Tan T. J. (1993) The importance of creep and time-dependent dilatancy as revealed from case records in China, in *Comprehensive Rock Engineering* (J. A. Hudson, ed.). Vol. 3, Ch. 31, 709–744.

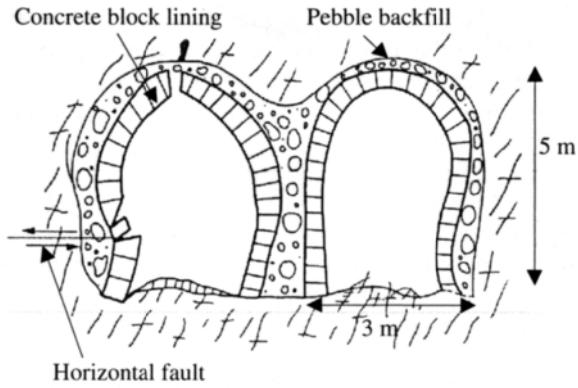

The tunnel axes are oriented perpendicular to the high intraplate horizontal tectonic stress, σ_H. The tunnel deformations have been described[5] as follows:

"Directly after excavation, the sidewalls started to bulge, horizontal cracks occurred which were growing in width and length; bottom heave was obvious. These processes increased in intensity with time. Void formation in the dilatancy process increasing with time leads to serious overall weakening of the rock structure; in addition it is aggravated by the suction and seepage of underground water. The horizontal displacements... were in the order of 50 cm within 90–150 days with an average rate of 5.4 mm/day. Usually the inwards motion of the corner areas near the bottom are largest, whereas the roof-top moved upwards so gradually the tunnel cross-section is squeezed into the 'peach' form... Bottom upheavals at some locations were about 40 cm within 131 days. Serious lateral motions of one sidewall have been observed."

Explain these observations in terms of the basic mechanisms involved.

A13.10 The observations are explained as follows.

"Directly after excavation, the sidewalls started to bulge, horizontal cracks occurred which were growing in width and length; bottom heave was obvious."

Firstly, consider the basic circumstances. The tunnels are located at 430 m depth so, knowing that 40 m depth $\approx$ 1 MPa, the vertical stress component will be about 430/40 $\approx$ 11 MPa. Also, we know that the tunnel axes are perpendicular to the maximal horizontal stress component, an orientation which causes the highest stress concentrations around the boundary of the excavations. Moreover, we can expect the maximal horizontal stress component to have a significantly greater value than the vertical stress component, thus causing the highest compressive stress concentrations to be located in the roof and floor.

Clearly, the ratio of rock stress to rock strength is high enough to cause significant displacements. The use of the words 'bulge' and 'bottom heave' to describe the sidewall and floor movements before the lining

was installed implies that the rock was being squeezed *en masse* into the excavation. The horizontal cracks could have developed as a result of the granite structure, or because the horizontal stress was so high that a tensile stress developed at the axis level (although such tensile stresses in fractured rock are unlikely).

"These processes increased in intensity with time. Void formation in the dilatancy process increasing with time leads to serious overall weakening of the rock structure; in addition it is aggravated by the suction and seepage of underground water. The horizontal displacements... were in the order of 50 cm within 90–150 days with an average rate of 5.4 mm/day."

The fact that the processes increased in intensity with time implies that the rock mass in the direct vicinity of the tunnels was deteriorating and hence becoming even more susceptible to the action of the rock stresses. The rock mass — composed of heavily fractured granite and containing faults — is below the water table, which means that water will readily flow into the tunnels. The tunnels themselves have a concrete block lining with pebble backfill, which will be relatively permeable and so will not prevent this water flow. The movement of ground water through the rock mass towards the tunnels would therefore aggravate the time-dependent degradation.

"Usually the inwards motion of the corner areas near the bottom are largest, whereas the roof-top moved upwards so gradually the tunnel cross-section is squeezed into the 'peach' form... Bottom upheavals at some locations were about 40 cm within 131 days. Serious lateral motions of one sidewall have been observed."

The inward motion of the corner areas near the bottom was largest because the major principal stress is acting horizontally and the lining is not continuous across the floor of the tunnels. If the tunnels had been unlined, the roof would probably have been squeezed downwards, i.e. into the excavation, in the same way as the floor was being squeezed upwards. Thus, the lining must be having a significant effect in transferring the lateral force resulting from the horizontal stress into the roof and floor: the roof is pushed upwards, and the corner at the floor is pushed inwards. If the tunnels are not behaving symmetrically, as evidenced by the fact that serious lateral motions of one sidewall have been observed, it is likely that the fracturing in the granite is neither homogeneous nor isotropic, and that the rock mass is weaker on one side of the tunnels.

13.3 Additional points

All the subjects that have been covered in Chapters 4–13 — *in situ* stress, elasticity, the deformability, strength and failure of intact rock, fractures and rock masses, permeability, anisotropy and inhomogeneity, rock mass classification, *and* time dependency — can be incorporated into numerical programs, as demonstrated by the finite element stability

analyses (Wittke, 1999[6]) for the tunnels of the high-speed German railway line in which the elastoviscoplastic behaviour of both intact rock and fractures was incorporated. However, time dependency is a difficult subject and, although other programs can potentially incorporate time dependency, such as the 'tunnel support modeller' add-on to the FLAC program[7] which uses the Panet (1993)[8] convergence-confinement tunnel analysis, time-dependent behaviour is difficult to incorporate into rock mechanics modelling and is generally ignored. For example, the value of the design life, say 120 years, is not explicitly used in modelling calculations.

The reasons for the difficulty in incorporating time dependency into modelling for rock engineering design are that the mechanics involved in the rheology of rocks and rock masses is not fully understood, the range of strain rates in engineering applications is wide, ranging from blasting strain rates to creep strain rates, and it is difficult to establish the parameters associated with time-dependent behaviour.

[6] Wittke W. (1999) Stability analysis of tunnels of the new high speed Cologne–Rhine/Main Railway Line. *ISRM News Journal*, **5**, 3, 26–33.

[7] Distributed by ITASCA, software@itascag.com and www.itasca.com

[8] Panet M. (1993) Understanding Deformations in Tunnels, in *Comprehensive Rock Engineering* (J. A. Hudson, ed.). Vol. 1, Ch. 27, pp. 663–690.